Available online at www.sciencedirect.com
SCIENCE DIRECT
Thermochimica Acta 447 (2006) 190–196
thermochimica acta
www.elsevier.com/locate/tca

Kinetics of thermal degradation applied to starches from different botanical origins by non-isothermal procedures

Luciana S. Guinesi [a,*], Alessandra L. da Róz [a], Elisângela Corradini [b], Luiz Henrique C. Mattoso [b], Eliangela de M. Teixeira [a], Antonio A. da S. Curvelo [a]

[a] *Instituto de Química de São Carlos, Universidade de São Paulo, Av. do Trabalhador São-carlense, 400, CEP 13566-590, São Carlos, SP, Brazil*
[b] *Embrapa Instrumentação Agropecuária, C.P. 741, São Carlos 13560-970, SP, Brazil*

Received 23 February 2006; received in revised form 1 June 2006; accepted 7 June 2006
Available online 13 June 2003

Abstract

Amylose content, crystallinity, morphology and the kinetic of thermal degradation to starches from different botanical origins are described based on XRD, SEM, DSC and TG/DTG curves. Applying the non-isothermal isoconversional Wall–Flynn–Ozawa method on the TG/DTG curves average activation energy ($0.10 \leq \alpha \leq 0.70$) $E = 144.1 \pm 9.8$, 171.6 ± 14.6, 158.3 ± 7.4 and $159.4 \pm 15\,\mathrm{kJ\,mol^{-1}}$ could be obtained for thermal degradation of corn, rice, potato and cassava starches, respectively. From E values and the generalized time θ, the Sesták–Berggren (SB) in which $f(\alpha) = \alpha^m(1-\alpha)^n$ seems to be most suitable kinetic model in describing physicogeometrically the thermal degradation for the samples regardless of its botanical origins. The determination of the kinetic exponents m and n allows to obtain the pre-exponential factor ($0.2 \leq \alpha \leq 0.8$) $\ln A = 8.8$, 10.4, 9.2 and $8.9\,\mathrm{min^{-1}}$ for corn, rice, potato and cassava starches, respectively. There were not significant differences between values of the kinetic triplet of the starches, indicating that, despite structural differences, these had little influence on the thermal degradation process of the starches.

Keywords: Kinetics; Starches; Thermal degradation; Flynn–Wall–Ozawa method; Sesták–Berggren model

1. Introduction

1.1. Starches

Starch is a biopolymer present in seeds, roots and stems of different plants, including corn, rice, potato and cassava. The amylose and amylopectin are the main constituents of the starches. The amylose is predominantly a linear polymer of α-$(1 \rightarrow 4)$-linked glucose whereas amylopectin is a highly branched polysaccharide consisting of α-$(1 \rightarrow 4)$-linked glucose with α-$(1 \rightarrow 6)$-linkages at the branch points [1].

The crystallinity of the starches granules depends mainly on its crystalline amylopectin content that varies with the botanical origin. Crystalline patterns of the common native starches can be classified into three categories: the cereal starches as A type, the tuber and maize starches as B type and bean and other root starches as C type, which it is an intermediate between A type and B type [2]. Although the starches from different botanical origins have identical structural units, the amylose and amylopectin contents exercise great influence on its physical and chemical properties.

The conventional processing techniques of starches used in the food-processing industries and preparation of thermoplastic materials are carried out at relatively high temperatures [3]. The extension of the molecular structure degradation in the starches depends upon the temperature and time employed that have great influence on its physical properties and technological applications [4]. So far, no systematic study has been carried out to evaluate the kinetic of thermal degradation of starches from corn, rice, potato and cassava.

In this sense, the main objective of the present work is the evaluation of the amylose content, crystallinity, morphology and the kinetic parameters activation energy, E, pre-exponential factor, A, and the kinetic model, $f(\alpha)$, regarding the thermal degradation of starches from corn, cassava, rice and potato based on X-ray diffraction (XRD), scanning electron microscopy (SEM), differential scanning calorimetry (DSC) and thermogravimetry/differential thermogravimetry (TG/DTG) curves.

* Corresponding author. Tel.: +55 16 3373 9958; fax: +55 16 3373 9987.
E-mail address: luguinesi@yahoo.com.br (L.S. Guinesi).

0040-6031/$ – see front matter © 2006 Elsevier B.V. All rights reserved.
doi:10.1016/j.tca.2006.06.002

The kinetic aspects for E determination using the isoconversional method of Flynn–Wall and Ozawa has widely been described [5–10] and they are not presented here. Differently, the $f(\alpha)$ determination is a relatively new approach whose method is described below. The A kinetic parameter was obtained from $f(\alpha)$.

1.2. Kinetic model determination

The mathematical description of the data from a single step solid state degradation is usually defined in terms of a kinetic triplet: activation energy, E, pre-exponential factor, A, and an algebraic expression of the kinetic model as a function of the fractional conversion α, $f(\alpha)$, which can be fitted to the experimental data as follows [5]:

$$\frac{d\alpha}{dt} = A \exp\left(-\frac{E}{RT}\right) f(\alpha) \quad (1)$$

For dynamic data obtained at a constant heating rate, $\beta = dT/dt$, this new term is inserted in Eq. (1) to obtain:

$$\frac{d\alpha}{dT} = \frac{A}{\beta} \exp\left(-\frac{E}{RT}\right) f(\alpha) \quad (2)$$

where R is the gas universal constant ($8.314\,J\,K^{-1}\,mol^{-1}$).

Compared with isothermal experiments, non-isothermal runs are more convenient to carry out because it is not necessary to perform a sudden temperature jump of the sample at the beginning [11].

Once the activation energy has been determined, it is possible to find the kinetic model that best describes measured set of thermogravimetric data.

The kinetic rate equation at infinite temperature is obtained by using the concept of the generalized time, θ, introduced by Ozawa [6,12]:

$$\theta = \int_0^t \exp\left(-\frac{E}{RT}\right) dt \quad (3)$$

where θ denotes the reaction time taken to attain a particular α at infinite temperature. First differentiation of Eq. (3) gives [13]:

$$\frac{d\theta}{dt} = \exp\left(-\frac{E}{RT}\right) \quad (4)$$

Combining Eq. (1) with Eq. (4) the following expression is obtained [13–15]:

$$y(\alpha) = \frac{d\alpha}{d\theta} = A f(\alpha) \quad (5)$$

where $d\alpha/d\theta$ corresponds to the generalized reaction rate obtained by extrapolating the reaction rate in real time, $d\alpha/dt$, to infinite temperature [13,14].

The integrated form of Eq. (5) after rearrangement gives [14]:

$$g(\alpha) = \int_0^\alpha \frac{d\alpha}{f(\alpha)} = A \int_0^\theta d\theta = A\theta \quad (6)$$

By combining Eqs. (5) and (6), we obtain the following general expression for the $z(\alpha)$ function [16]:

$$z(\alpha) = \left(\frac{d\alpha}{d\theta}\right) \theta = f(\alpha) g(\alpha) \quad (7)$$

However, $y(\alpha)$ and $z(\alpha)$ requires the knowledge of θ which is defined by Eq. (3) that involves the time dependence of temperature. From the kinetic data under a linear heating rate of β, the value of θ at a given α can be defined as [14]:

$$\theta = \frac{1}{\beta} \int_0^T \exp\left(-\frac{E}{RT}\right) dT = \frac{E}{\beta R} \int_x^\infty \frac{\exp(-x)}{x^2} dx = \frac{E}{\beta R} p(x) \quad (8)$$

The function $p(x)$, where $x = E/RT$, cannot be expressed in a closed form, although several convergent series exist for its approximation. For example, the fourth rational Senum and Yang [17] corrected by Flynn [9], allows an accuracy of better than 10^{-5}% for $E/RT = 20$. So, $p(x)$ can be expressed by

$$p(x) = \frac{e^{-x}}{x} \pi(x) \quad (9)$$

where

$$\pi(x) = \frac{x^3 + 18x^2 + 86x + 96}{x^4 + 20x^3 + 120x^2 + 240x + 120} \quad (10)$$

Because the $y(\alpha)$ and $z(\alpha)$ functions are invariable with respect to temperature or heating rate, being quite sensitive to subtle changes in the kinetic model $f(\alpha)$, they can be conveniently used as suitable tools for kinetic model determination [15].

2. Experimental

2.1. Materials

The starches used in this work were a commercial products obtained from corn and cassava (Corn Produtos do Brasil), rice (L. Ferenczi Industria e Comércio LTDA) and potato (Yoki Alimentos S.A.). The moisture content was about 10% for all starches. L-α-Lysophosphatidylcholine (LPC) from egg yolk (Sigma) was used without further treatment.

2.2. Differential scanning calorimetry

The DSC measurements were performed in a DSC-50 modulus from Shimadzu. Indium metal (99.99%) has been used to calibrate the DSC modulus in relation to temperature and enthalpy. The DSC curves were performed under dynamic nitrogen atmosphere ($20\,mL\,min^{-1}$) using starches sample mass around 3 mg and heating rate at $10\,°C\,min^{-1}$. Accurately weight samples of starches from corn, rice potato and cassava (±0.1 mg) and 10.00 μL of LPC aqueous solution (2%, w/v) were placed into an aluminum high pressure sample holder. The mixture was stirring and stored for 1 h to assure its stabilization. An aluminum sample holder with 10.00 μL of distilled water was used as reference. The sample holders were covered and the first

run was performed heating the samples from 35 to 160 °C at 10 °C min^{-1} with an isothermal for 2 min at 160 °C and cooled to 25 °C at 5 °C min^{-1}. The second run was performed just as the first one.

2.3. X-ray diffraction

The X-ray powder diffraction patterns were obtained using a Rigaku X-ray diffractometer with Cu Kα (λ = 1.542 Å) radiation, submitted to 20 kV/100 mA, step of 1000 min^{-1} and exposed to radiation from 3 to 40° (2θ).

2.4. Scanning electron microscopy

The scanning electron microscopies were performed using a microscope Leo 440. The samples were dispersed in acetone and agglutinated with a carbon ribbon adhesive, dried under reduced pressure at 90 °C for 10 h and sputter coated with a 20 nm gold layer.

2.5. Thermogravimetry (TG)

Thermogravimetry (TG) and differential thermogravimetry (DTG) were performed in a TA 50 modulus from Shimadzu. The TG/DTG curves of the starches were carried out under dynamic nitrogen atmosphere (20 mL min^{-1}), platinum crucible, sample mass around 7 mg and heating rates of 5, 10, 15 and 20 °C min^{-1} from 25 to 800 °C.

3. Results and discussion

3.1. Starch granule properties and compositions

Values of the amylose content, based on the method described by Mestre et al. [18], were obtained from the DSC curves presented in Fig. 1. The cooling DSC curves at the second run show exothermic peaks at 92.7, 93.3, 93.8 and 94.3 °C attributed to the complexes between LPC and the amylose from corn, rice, potato and cassava, respectively.

The starches amylose content can be calculated using the following equation:

$$\text{amylose content (\%)} = 100 \times \frac{\Delta H_1}{\Delta H_2} \quad (11)$$

where ΔH_1 is the enthalpy associated to the formation of the complex at the second cooling and ΔH_2 is the standard enthalpy for amylose, 25 J g^{-1} [19]. Based on the change in enthalpy, the amylose contents are 28, 15, 15 and 14% for corn, rice, potato and cassava, respectively.

The DSC curves indicate a reversible process after various runs. However, the constancy in ΔH_1 at the second run indicates the equilibrium condition because in the first heating perhaps all the starch has not solubilized in water until the end. Endothermic peaks in the 100–115 °C (not shown) can be attributed to the non-equilibrium melting of the complexes due to the partial recrystallization of the amylose [18] requiring two runs for a quantitative approach.

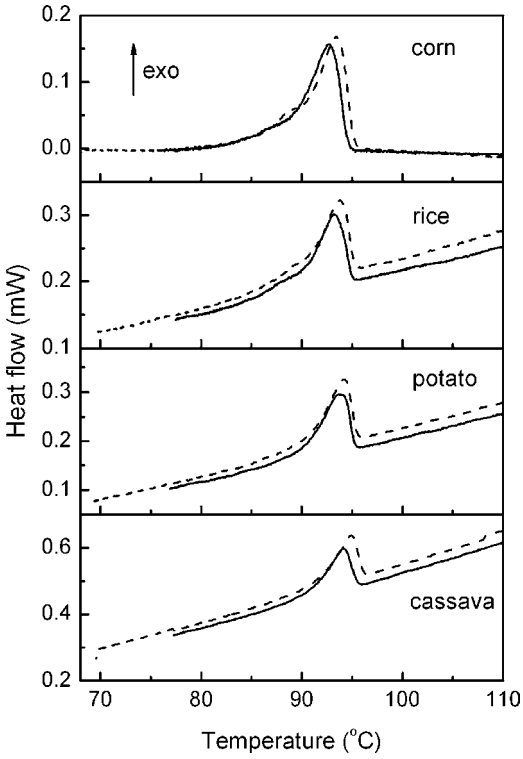

Fig. 1. First (– – –) and second (—) cooling DSC curves to the starches under nitrogen atmosphere at 5 °C min^{-1}.

The X-ray powder diffraction patterns to the starches are presented in Fig. 2. A similar crystalline pattern can be observed for corn and rice starches that are typical to the starches A type, whereas potato has a B type pattern and cassava show a C type according to data in the literature [20]. Values of the crystallinity index (X_c) were obtained based on the method described by Hulleman et al. [21] using the following equation:

$$X_c = \frac{H_c}{H_c + H_a} \quad (12)$$

where H_c and H_a are the intensities for the crystalline and amorphous profiles with typical baselines at a value of 2θ between 17° and 18° as shown in Fig. 2, respectively. The crystallinity indexes are 0.44, 0.53, 0.55 and 0.50 for corn, rice, potato and

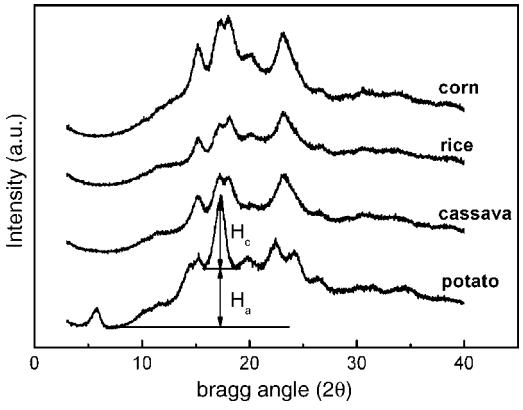

Fig. 2. X-ray diffraction patterns to the starches. H_a and H_c are the amorphous and crystalline profiles, respectively.

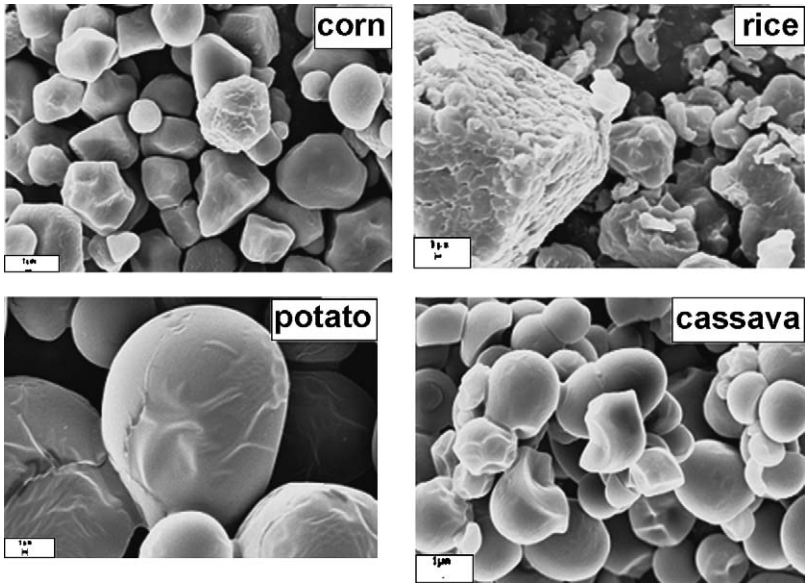

Fig. 3. Scanning electron microscopy to the starches.

cassava, respectively. The amylose and amylopectin are the main constituents of the starches whose contents are inversely proportional [22]. Since the granules crystallinity depends mainly on the crystalline amylopectin chains [2], the highest amylose content for corn justifies its lowest X_c value among the starches. Therefore, the starches from rice, potato and cassava show the proximity in X_c values due to its proximity in amylose contents.

The scanning electron microscopies for starches are presented in Fig. 3. Among the starches, potato shows the biggest granules, 20–33 μm, and rice has the smallest ones, 1.5–4.0 μm, aggregated into compound granules with diameters of 15–50 μm interval. Corn and cassava starches have similar granules sizes with diameters of 8.0–15 and 11–18 μm intervals, respectively.

The TG/DTG curves under nitrogen atmosphere at several heating rates for starches from corn, rice, potato and cassava presented a mass loss between 25 and 174 °C related to the water elimination, Fig. 4a and b. The second step between 274 and 374 °C can be related to the depolymerization and degradation of the starches in a non-oxidative process [23,24]. Pyrolysis of starches at 300 °C in a stream of nitrogen has been described to

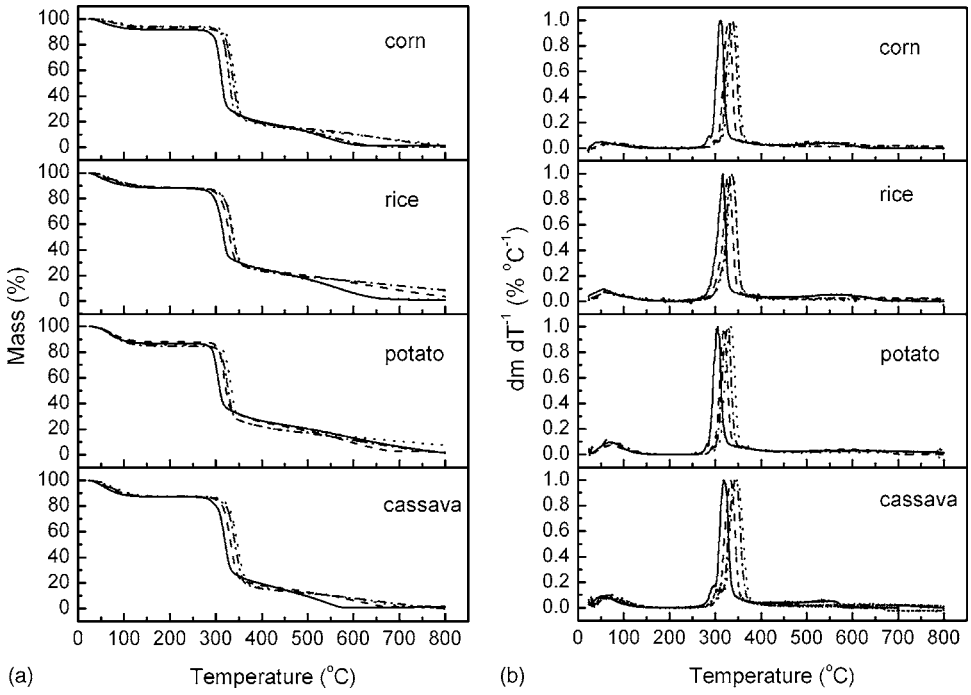

Fig. 4. (a) TG curves to the starches under nitrogen atmosphere at 5 °C min^{-1} (—), 10 °C min^{-1} (– – –), 15 °C min^{-1} (–·–·–) and 20 °C min^{-1} (· · ·). (b) DTG curves to the starches under nitrogen atmosphere at 5 °C min^{-1} (—), 10 °C min^{-1} (– – –), 15 °C min^{-1} (–·–·–) and 20 °C min^{-1} (· · ·).

give CO_2, CO, water, acetaldehyde, furan and 2-methyl furan [25,26]. For corn, levoglucosan is usually the main constituent of the decomposed products, besides complex gases and water liberated [27]. The third step may be ascribed to the total degradation of the intermediate products at 800 °C. A carbonaceous residue has been described for thermal degradation of corn at 500 °C under nitrogen atmosphere [23,24].

These curves were used for the evaluation of E, $f(\alpha)$ and A.

3.2. Calculation of the activation energy

The activation energy related to the second thermal event of the starches were obtaining applying the isoconversional method of Flynn, Wall and Ozawa [5–9] to the mass losses defined by TG/DTG curves at 5, 10, 15 and 20 °C min^{-1} (Fig. 4a and b). The reaction limits employed are presented in Table 1.

To each fixed fractional conversion, $0.10 \leq \alpha \leq 0.70$, the activation energy, E, could be calculated from the slope of $\ln \beta$ *versus* $1000/T$ (K^{-1}) plot. The obtained results must be within the limit $28 \leq E/RT \leq 50$ in order to permit to be use the Doyle approximation to $p(x)$ [28]. According to the isoconversional method, the reaction rate at a constant extent of conversion is only a function of temperature and the independence of E from α and T may be tested by determining E at various α [8,10]. The E *versus* α plots to the starches are presented in Fig. 5. The constancy of E in relation to α indicates the applicability of the Flynn–Wall–Ozawa method on thermal degradation of the starches.

The E medium values (Table 1) fall in the same range as that reported for other natural polymers [29–31]. There is no a coherent correlation between the activation energy and the crystallinity for the starches. Morphologic aspects could be the reason for the activation energy behavior such as for rice that presented the highest E associated to its intermolecular interactions between individual granules that are aggregated in the starch (Fig. 3).

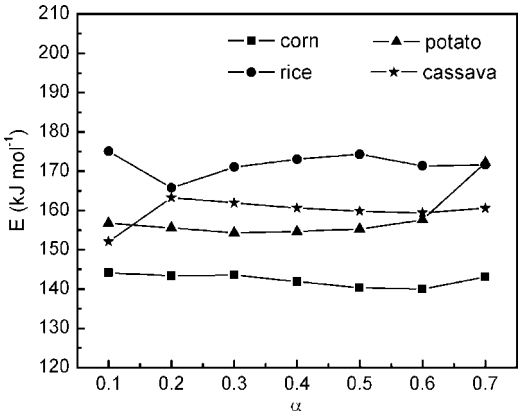

Fig. 5. Dependence of the activation energy on the extent of conversion obtained from the isoconversional method regarding the thermal decomposition to the starches.

3.3. Determination of the kinetic model and pre-exponential factor

To the data from TG/DTG curves at 15 °C min^{-1} under nitrogen atmosphere, the physicogeometric mechanism or kinetic model, $f(\alpha)$, to the second step of thermal degradation of the starches has been determined. For this purpose, the kinetic rate equation at infinite temperature, Eq. (3), obtained by using the concept of generalized time θ, seems to be very useful [6,12]. However, this determination can be reached by extrapolating the kinetic data recorded in real time under any temperature profile, $d\alpha/dT$, to infinite temperature, $d\alpha/d\theta$, which corresponds to the generalized reaction rate, Eq. (5) [13,14]. The extrapolation requires the knowledge of α and θ. The fractional conversion α can be calculated by partial integration of DTG curve [16]. The generalized time θ can be calculated using Eqs. (8)–(10) [14].

Knowing α and θ, it is possible to define the $y(\alpha)$ and $z(\alpha)$ functions calculated by Eqs. (5) and (7) whose shape and maximum values can be used as a guide in the kinetic model

Table 1
Reaction limits taken from TG/DTG curves to obtain the kinetic parameters E and A regarding the second step of thermal degradation to the starches

Starch	Heating rate (°C min^{-1})	Temperature range (°C)	Mass loss (%)	E (kJ mol^{-1})	$\ln A$ (min^{-1})[a]
Corn	5	290–347	67.5	144.1 ± 9.8	8.8
	10	302–351	67.2		
	15	308–365	67.6		
	20	310–374	67.0		
Rice	5	274–350	61.3	171.6 ± 14.6	10.4
	10	281–359	61.6		
	15	288–369	61.5		
	20	291–371	61.0		
Potato	5	285–346	57.0	158.3 ± 7.4	9.2
	10	294–349	56.4		
	15	301–352	56.1		
	20	304–361	56.0		
Cassava	5	297–344	67.0	159.4 ± 15.0	8.9
	10	299–357	67.7		
	15	300–368	67.2		
	20	308–374	66.8		

[a] The $\ln A$ values are obtained from the SB model.

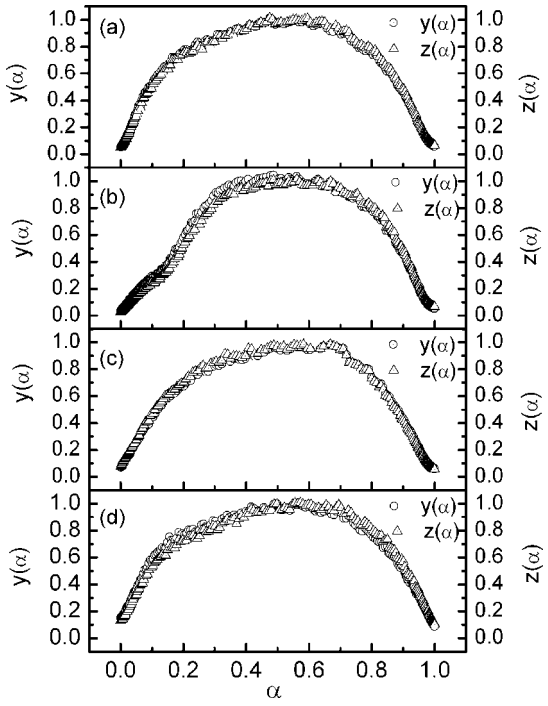

Fig. 6. The normalized $y(\alpha)$ and $z(\alpha)$ functions regarding the second step of thermal degradation to the corn (a), rice (b), potato (c) and cassava (d) starches.

determination [15,32,33]. Fig. 6 presented the $y(\alpha)$ and $z(\alpha)$ functions normalized within the $\langle 0, 1\rangle$ interval regarding the second thermal degradation event of the corn, rice, potato and cassava starches. The $z(\alpha)$ function presented its maximum, α_z^*, located at 0.52, 0.54, 0.56, and 0.52 for corn, rice, potato and cassava, respectively. The $y(\alpha)$ function presented its maximum, α_y^*, located at 0.48, 0.52, 0.53, and 0.52 for corn, rice, potato and cassava, respectively.

If $y(\alpha)$ function exhibits its maximum in $0 < \alpha_y^* < \alpha_p$ interval (where α_p is the fractional extent corresponding to the maximum rate $d\alpha/dt$), the Sesták–Berggren (SB) or Johnson–Mehl–Avrami (JMA) are the most probable kinetic models [15,32,33].

The JMA kinetic model was developed to describe the formal theory of nucleation and growth and it can be applied to the description of non-isothermal TA data when the entire nucleation process takes place during early stages of the transformation and becomes negligible afterwards [34].

However, the validity of the JMA kinetic model can easily be verified by checking the maximum α_z^* that falls into the $0.61 \leq \alpha_z^* \leq 0.65$ interval [16]. For starches, α_z^* are shifted to lower values, which do not correspond to the JMA kinetic model. Therefore, the $y(\alpha)$ and $z(\alpha)$ functions satisfy the condition for SB model described by the kinetic equation $f(\alpha) = \alpha^m(1-\alpha)^n$. The kinetic parameters n and $\ln A$ can be calculated from the logarithmic form of Eq. (1) considering $f(\alpha) = \alpha^m(1-\alpha)^n$ that after rearrangement yields Eq. (13) [32,33]:

$$\ln\left[\left(\frac{d\alpha}{dt}\right)e^x\right] = \ln A + n\ln[\alpha^p(1-\alpha)] \quad (13)$$

where $x = E/RT$ and $p = \alpha_y^*/(1-\alpha_y^*)$. The slope of the linear dependence $\ln[(d\alpha/dt)e^x]$ *versus* $\ln[\alpha^p/(1-\alpha)]$ plot within the $0.2 \leq \alpha \leq 0.8$ interval yields $n = 0.60$, 1.17, 0.65, 0.52 for corn, rice, potato and cassava starches respectively and the linear intercept yields $\ln A$. The $\ln A$ values for the starches are presented in Table 1. The relation $m = pn$ yields $m = 0.55$, 1.27, 0.73, 0.56 for corn, rice, potato and cassava, respectively [32,33,35,36].

The increasing value of the kinetic exponent m indicates a more important role of the product on the overall kinetics with an autocatalytic behavior. It seems that a higher value of the kinetic exponent $n > 1$ means increasing complexity of the process and can be caused, for example, by the influence of surface nucleation. In fact, the two-parameter SB model includes the JMA as a special case whose applicability involves a narrowest limit for α_y^* and α_z^* values in relation to the SB [15]. However, the physical meaning attributed for m and n should not go beyond of those described above, unless more detailed conclusions concerning the degradation mechanism should be based on other types of complementary evidence, including microscopic observations and all other relevant information [16].

Knowing the $\alpha - T$ dependence and the kinetic triplet: E, $\ln A$ and $f(\alpha)$, the simulated $d\alpha/dT$ *versus* T plots can be calculated using Eq. (2) whose proximity with the experimental DTG curves confirms the SB as the kinetic model in describing physicogeometrically the thermal degradation for all starches. Fig. 7 presents the simulated and experimental DTG curves at $15\,^{\circ}C\,min^{-1}$ normalized within the $\langle 0, 1\rangle$ interval. The thermal stability of the starches exercise little influence on the activation energy, such as for cassava and rice starches whose E values (Table 1) have no directly proportional correlation with

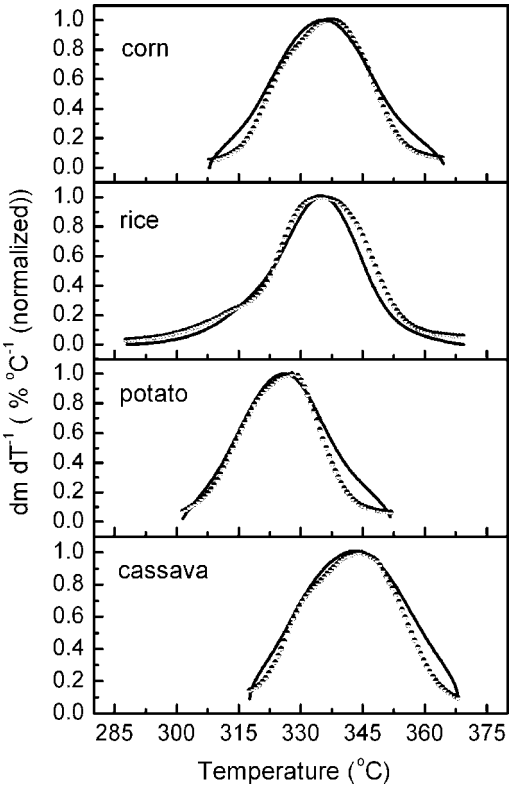

Fig. 7. The experimental (◓) and simulated (—) DTG curves at $15\,^{\circ}C\,min^{-1}$ in agreement with the SB kinetic model regarding the thermal degradation of the starches.

its thermal stabilities (Figs. 4b and 6). In this sense, the kinetic parameters E, A and n, m could be compensated between them for fitting the experimental curve.

4. Conclusions

Despite the strong dependence of kinetic on the experimental conditions in a dynamic procedure, it can be seen from the resemblance between the simulated and experimental DTG curves, that the kinetic triplet: E, $\ln A$ and $f(\alpha)$, could be obtained satisfactorily. The autocatalytic SB kinetic model was successfully applied to all samples indicating the complexity in thermal degradation to the starches. There are not significant differences between values of the kinetic triplet of the starches, indicating that, despite structural differences, these had little influence on the thermal degradation process of the starches.

Acknowledgment

The authors acknowledge the Brazilian agencies FAPESP and CNPq for financial support.

References

[1] J.M.V. Blanshard, in: T. Galliard (Ed.), Starch: Properties and Potential, John Wiley, Chichester, 1987, pp. 16–54.
[2] J.J.G. Van Soest, J.F.G. Vliegenthart, Trends Biotechnol. 15 (1997) 208.
[3] E.M. Teixeira, A.L. da Roz, A.J.F. Carvalho, A.A.D. Curvelo, Macromol. Symp. 229 (2005) 266.
[4] P. Aggarwal, D. Dollimore, Instrum. Sci. Technol. 27 (1992) 191.
[5] M.E. Brown, D. Dollimore, A.K. Galwey, Reaction in the Solid State, vol. 22: Comprehensive Chemical Kinetics, Elsevier, Amsterdam, 1980, p. 22.
[6] T. Ozawa, Bull. Chem. Soc. Jpn. 38 (1965) 1881.
[7] J.H. Flynn, L.A. Wall, J. Res. Nat. Bur. Stand. A 70 (1966) 487.
[8] J.H. Flynn, L.A. Wall, J. Polym. Sci. Pt. B 4 (1966) 323.
[9] J.H. Flynn, Thermochim. Acta 300 (1997) 83.
[10] S. Vyazovkin, C.A. Wight, Int. Rev. Phys. Chem. 17 (1998) 407.
[11] S. Vyazovkin, C.A. Wight, Thermochim. Acta 340/341 (1999) 53.
[12] T. Ozawa, Thermochim. Acta 100 (1986) 109.
[13] N. Koga, Thermochim. Acta 258 (1995) 145.
[14] F.J. Gotor, J.M. Criado, J. Malek, N. Koga, J. Phys. Chem. A 104 (2000) 10777.
[15] J. Málek, T. Mitsuhashi, J.M. Criado, J. Mater. Res. 16 (2001) 1862.
[16] J. Málek, Thermochim. Acta 355 (2000) 239.
[17] G.I. Senum, R.T. Yang, J. Therm. Anal. 11 (1977) 445.
[18] C. Mestre, F. Matencio, B. Pons, M. Yajid, G. Fliedel, Starch/Starke 48 (1996) 2.
[19] C. Gérard, C. Barron, P. Collona, V. Planchot, Carbohydr. Polym. 44 (2001) 19.
[20] P. Collona, A. Buleon, C. Mercier, in: T. Galliard (Ed.), Starches: Properties and Potential, John Wiley, Chichester, 1987, p. 79.
[21] S.H.D. Hulleman, M.G. Kalisvaart, F.H.P. Janssen, H. Feil, J.F.G. Vliegenthart, Carbohydr. Polym. 39 (1999) 351.
[22] N.H.W. Cheetham, L. Tao, Carbohydr. Polym. 33 (1997) 251.
[23] P. Aggarwal, D. Dollimore, K. Heon, J. Therm. Anal. 50 (1997) 7.
[24] P. Aggarwal, D. Dollimore, Thermochim. Acta 319 (1998) 17.
[25] D.J. Bryce, C.T. Greenwood, Starke 15 (1963) 166.
[26] D.J. Bryce, C.T. Greenwood, Starke 15 (1963) 285.
[27] C.T. Greenwood, Adv. Carbohydr. Chem. 22 (1967) 483.
[28] C.D. Doyle, J. Appl. Polym. Sci. 5 (1961) 445.
[29] M.A. Villetti, J.S. Crespo, M.S. Soldi, A.T.N. Pires, R. Borsali, V. Soldi, J. Therm. Anal. Cal. 67 (2002) 295.
[30] Z. Stojanovic, L. Katsikas, I. Popovic, S. Jovanovic, K. Jeremik, Polym. Degrad. Stab. 87 (2005) 177.
[31] E. Corradini, E.A.G. Pineda, A.A.W. Hechenleitner, Polym. Degrad. Stab. 66 (1999) 199.
[32] J. Málek, J. Sesták, F. Rouquerol, J. Rouquerol, J.M. Criado, A. Ortega, J. Therm. Anal. 38 (1992) 71.
[33] J. Málek, Thermochim. Acta 200 (1992) 257.
[34] J. Málek, Thermochim. Acta 267 (1995) 61.
[35] L.S. Guinesi, C.A. Ribeiro, M.S. Crespi, A.M. Veronezi, Thermochim. Acta 414 (2004) 35.
[36] G.C.A. Amaral, M.S. Crespi, C.A. Ribeiro, M.Y. Hikosaka, L.S. Guinesi, A.F. Santos, J. Therm. Anal. Cal. 79 (2005) 375.